Spin-polarized current switching of a Co thin film nanomagnet

F. J. Albert, J. A. Katine,[a] and R. A. Buhrman[b]
School of Applied and Engineering Physics, Cornell University, Ithaca, New York 14853

D. C. Ralph
Laboratory of Atomic and Stolid State Physics, Cornell University, Ithaca, New York 14853

(Received 12 June 2000; accepted for publication 7 October 2000)

A thin film Co nanomagnet in the shape of an elongated hexagon has been incorporated in a vertical device structure consisting of the nanomagnet and a thin Cu spacer layer formed on top of a thick Co film. The spin-polarized current flowing between the nanomagnet and the Co film is used to abruptly switch the magnetic alignment of the nanomagnet relative to that of the thick Co layer by the transfer of spin angular momentum from the conduction electrons to the nanomagnet moment. The shape anisotropy in the nanomagnet promotes the single domain behavior required for nonvolatile memory applications. © *2000 American Institute of Physics.* [S0003-6951(00)04549-6]

Recently attention has been given to high-current-density effects in magnetic thin film multilayers, motivated by both the physics involved and the possibility of novel, direct-current-switched magnetic memory devices. If a magnetic bit could be switched by the current passing through it, rather than by some external magnetic field, the design of high density nonvolatile memory would be greatly simplified. In current-perpendicular-to-the-plane (CPP) structures, two distinct physical mechanisms may allow the relative orientation of ferromagnetic layers (and, hence, the device resistance) to be controlled by the current traversing the layers. First, the magnetic self-field created by a large current can cause domain realignment into a vortex state.[1,2] In this letter, we focus on an alternative mechanism through which the current in the device can affect its magnetization: the torque exerted on the magnetic moment of a thin ferromagnetic film by the transfer of angular momentum from a spin-polarized current traversing the film.[3–6] As a result of this torque, at high current density a spin-polarized current can stimulate spin waves[7–9] or even full magnetization reversal of a small nanomagnet.[8–10] The self-field and the spin-transfer effects are in competition and can be observed in the same current ranges or in different current ranges, depending on the magnetic parameters of the materials and on the diameter of the nanomagnet, d. Self-field effects scale as $1/d$, while spin transfer effects scale as $1/d^2$, so spin-transfer effects become more important in smaller devices.

In circular nanopillars fabricated from Co(10 nm)/Cu(6 nm)/Co(2.5 nm) trilayer films, spin-transfer switching of the thin Co layer has been observed for $d \leqslant 200\,\text{nm}$.[2,9] However, in the previous CPP spin-transfer study,[9] the circular geometry employed resulted multidomain behavior during the transitions. This acts to extend the switching transition over a range of applied current and makes the device performance less than optimal, both for applications and for detailed study of the spin-transfer phenomena. Magnetization studies of nanomagnet arrays[11] have shown that the introduction of shape anisotropy can result in single domain behavior in sufficiently small thin film structures. Here we report results obtained with the use of an elongated-hexagon geometry that introduces a shape anisotropy into a thin film nanomagnet in close electrical proximity to a continuous ferromagnetic layer. The nanomagnet is fabricated in a nanopillar CPP configuration so that spin-transfer switching can be induced and the resultant orientation of the nanomagnet determined from the resistance of the nanopillar. The result is single-domain-like spin-transfer switching behavior.

Figure 1(a) shows a cross-sectional schematic of the nanopillar devices used in these experiments. We fabricated these spin-transfer devices by first sputtering a Cu(80 nm)/Co(40 nm)/Cu(6 nm)/Co(2.5 nm)/Au(10 nm) multilayer onto an oxidized Si substrate. The 80 nm Cu base layer served as the bottom electrode and the 40 nm Co base layer served as the fixed ferromagnet and spin polarization source. Electron beam lithography, thermal evaporation, and lift-off were used to pattern Au nanostructures in the shape of elongated hexagons onto the Au surface. Each of these Au nanostructures then served as an Ar ion mill mask that defined the nanopillar structure. The mill was timed to stop just after reaching the bottom Co layer, while leaving unpatterned, or nearly so. A scanning electron microscopy image of the device at this stage in the fabrication process is shown in Fig. 1(b). The final device dimensions of the nanomagnet were $\sim 60\,\text{nm} \times 130\,\text{nm}$, with the long ends of the nanomagnet tapering to a semipoint as shown in the figure. The devices were then planarized and the top electrode fabricated in the same manner as reported previously.[9]

The differential resistance dV/dI versus the applied magnetic field H for one of these Co/Cu/Co nanopillars is shown in Fig. 1(c) for one complete cycle of the applied field out to ± 1600 Oe and back to zero. For each pass of H through zero, the resistance of the nanopillar first jumps to a high state at low values of H, $\sim \pm 50$ Oe. These upward transitions in resistance result from the bottom, unpatterned Co layer changing its direction of magnetization. This leaves the Co layers in the antiparallel, high-resistance state. The

[a]Present address: IBM Almaden Research Center, 650 Harry Rd., San Jose, CA 95120.
[b]Electronic mail: rab8@cornell.edu

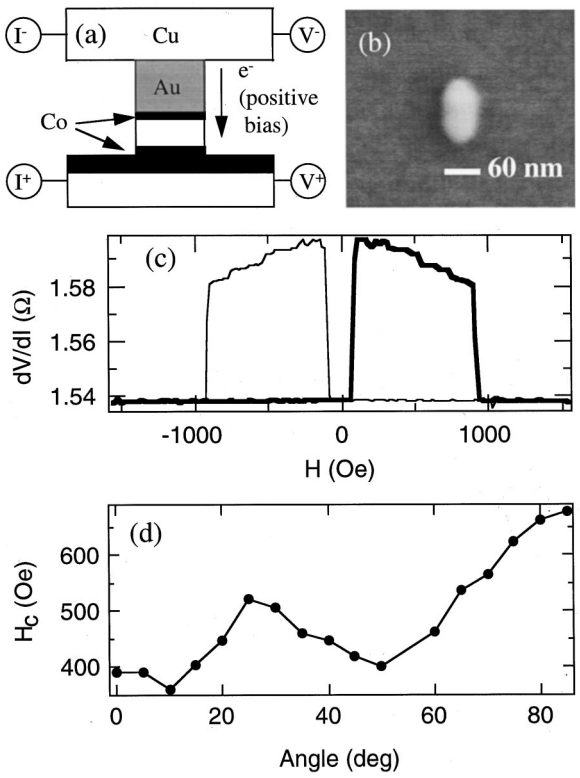

FIG. 1. (a) A schematic cross section of the nanopillar device used for the study of spin-transfer switching of Co nanomagnets. (b) A scanning electron micrograph of the Co nanomagnet before the top Au electrode covers the structure. (c) The differential resistance dV/dI as a function of magnetic field H applied parallel to the long axis of the nanomagnet. (d) The critical field H_c that is required to complete the transition to the fully aligned, low resistance state of a different nanopillar device as a function of the angle between the field and the long axis of the nanomagnet. The device in (d) has a different coercive field than the device in (c) due to nanofabrication variation.

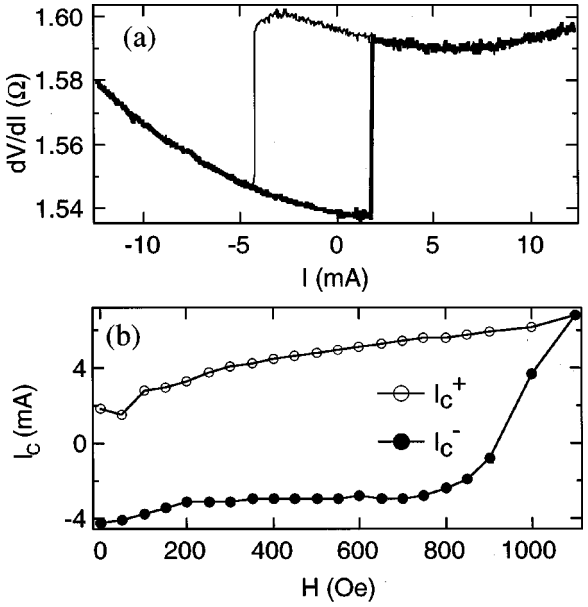

FIG. 2. (a) dV/dI of a nanopillar spin-transfer device as a function of the applied current through the device. The current is defined as positive when the spin-polarized electrons are flowing from the nanomagnet to the thick Co film. (b) The critical currents I_c^+ and I_c^- that switch the nanomagnet into, respectively, antiparallel and parallel alignment with the Co film as a function of H. This data was taken with H increasing from zero to its maximum value of 1100 Oe.

difference ΔR between the high and low resistance states is 59 mΩ. Past these upward transition points the device resistance gradually decreases with increasing $|H|$, indicating that a reversal domain has been nucleated and is partially propagating across the nanomagnet. At $\sim\pm 900$ Oe, the nanopillar jumps abruptly to the low-resistance state, completing the reversal of the nanomagnet's magnetization, past which point both magnetic layers are aligned with the field.

The magnetoresistance of these nanopillar devices can be used to study the magnetization behavior of individual patterned Co nanomagnets. Figure 1(d) shows the magnetic field required to switch of one of the nanomagnets into full alignment with the unpatterned Co layer, as measured as a function of the angle between the major axis of the hexagon and the applied field. We define the critical field H_c as that value where the resistance of the device abruptly completes the transition to the low resistance state. The critical field is roughly twice as large with H applied in-plane and perpendicular to the major (easy) axis of the elongated hexagon as compared to when H is parallel to the easy axis. For intermediate angles there is a local maximum in H_c at 25° and a local minimum at 50°. Thus the local maximum in H_c occurs when H is perpendicular to one of the sloped edges of the hexagon, and the minimum when H is parallel to another such edge. We note that for $\theta\sim 25°$, the resistance of the device is essentially unchanging until H_c is reached. This indicates that domains do not form in the nanomagnet at this field orientation until a complete transition is favorable.

The dV/dI response of the nanomagnet of Fig. 1(c) to spin-polarized currents flowing between it and the large Co film is shown in Fig. 2(a) for one complete cycle of the current from zero to ± 10 mA. Consistent with previous results, the transfer of spin-angular momentum to the nanomagnet by the electrons flowing from the thick Co layer forces the nanomagnet into parallel alignment (low-resistance state) above a critical current I_c^-. When the electrons flow from the nanomagnet, above a critical current I_c^+ the minority-spin-polarized electrons that are reflected back from the thick Co layer transfer sufficient spin-angular momentum to the nanomagnet to force it into antiparallel alignment (high-resistance state) with the Co layer. The ΔR between the parallel and antiparallel states established by the spin-transfer switching is identical to the ΔR measured with the field scan.

Both transitions between the two states of alignment of the nanomagnet are abrupt, with only a small precursor seen in the transition from the antiparallel to parallel state with increasing negative current, and none for the reverse transition. This behavior is typical of that seen in the elongated hexagon devices of this type that we have studied. The results obtained with these structures provide the means to more carefully examine theoretical models of spin-transfer switching than has previously been possible.

In the spin-transfer model,[4,9] the critical currents are given by

$$I_c^+ = \alpha e M \mathrm{Vol}[H + H_{\mathrm{an}} + 2\pi M]/hg(0),$$

$$I_c^- = \alpha e M \mathrm{Vol}[H - H_{\mathrm{an}} - 2\pi M]/hg(\pi).$$

Here $M = 1420\,\mathrm{emu/cm^3}$ for Co, Vol is the volume of the nanomagnet, and H_{an} is the anisotropy field of the nanomagnet, which we assume dominates over any dipolar and exchange field effects from the large Co layer. α is the phenomenological Gilbert damping parameter measured by ferromagnetic resonance to be 0.007 for Co.[12] $g(0)$ and $g(\pi)$ depend on the spin-dependent transmission probabilities of the ferromagnet-normal metal interfaces, the relative orientation ($0 =$ parallel, $\pi =$ antiparallel) of the nanomagnet, and any spin-flip scattering that may occur in the system.[4,6]

The zero field value of I_c^+ and I_c^- in Fig. 2(a) are 1.75 and -4.3 mA, respectively. For the 12 nanomagnet devices of the same nominal dimensions that we have studied to date, the average values of the critical currents are $I_c^+ = 2.3 \pm 0.8\,\mathrm{mA}$ and $I_c^- = -3.3 \pm 1.2\,\mathrm{mA}$. These results are consistent with the spin-transfer model if we take $g(0) = g(\pi) = 0.25$. The variation of the spin-transfer critical currents with H is illustrated in Fig. 2(b). In general we find that the critical current I_c^- for switching into parallel alignment varies comparatively weakly with field until H begins to approach the value that forces the nanomagnet into alignment in the absence of a current. In contrast I_c^+ typically increases, more or less linearly, by a factor of 2 or more by the time H_c is reached. This latter result is inconsistent with the equation given above by at least a factor of 10. We are pursuing experiments to ascertain whether this disagreement arises from a less than ideal behavior of the device, or is indicative of a basic deficiency in the spin-transfer model.

A problematic issue with magnetic thin film memory devices such as spin valves and magnetic tunnel junctions is a possible lack of consistency of the switching field of the free layer.[13] We have occasionally seen similar problems when switching these nanomagnet devices magnetically. This is illustrated in Fig. 3(a) where during the positive half cycle of a particular field scan, the device does not go into the high resistance state at all, yet on subsequent cycles of the field the behavior is as shown in Fig. 1(c). We suspect that this stems from domain-wall induced magnetostatic coupling[13] from the unpatterned, magnetically soft Co layer, which can explain why the behavior is only seen occasionally ($\sim$25%) during field sweeps as a particular domain wall orientation could be required to affect a premature switching of the nanomagnet. While this phenomenon could be a major problem for a field-switched nanomagnet memory device of this type, we find that switching via spin transfer is much more reliable. Figure 3(b) shows graphs of I_c^+ and I_c^- as measured for a series of current sweeps and plotted versus scan number. While there was some variation in the critical current, the device invariably switched into the antiparallel state for the positive-going current, and into the parallel state for the negative-going current. Thus, spin-transfer switching may have another intrinsic advantage over field switching for nanoscale magnetic memory devices.

In conclusion, we have fabricated CPP devices consisting of thin film Co nanomagnets with an elongated hexagon shape that are separated from a continuous Co film by a thin Cu spacer layer, and we have measured both the magnetoresistance and spin-transfer switching behavior of these individual nanomagnet structures. The critical currents for the spin-polarized switching are consistent with predictions of the spin-transfer model, but the lack of agreement with the predicted field dependence of the critical currents indicates that this phenomenon remains to be fully understood.

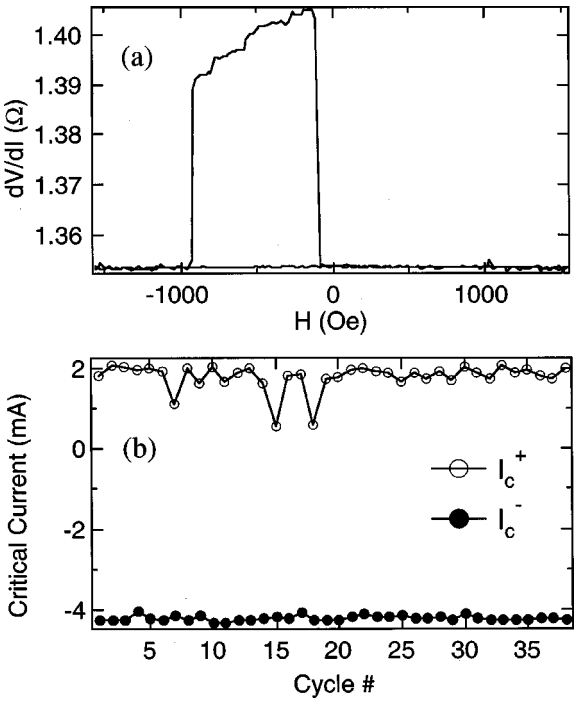

FIG. 3. (a) An example of the magnetoresistance behavior of a nanopillar device for a field cycle in which the nanomagnet switches at the same point that the thick Co film switches, presumably due to domain wall coupling. (b) The critical currents for spin-transfer switching for 30 cycles of the applied current to ± 5 mA.

The authors thank Roger Koch for a very helpful suggestion. This research was supported in part by the National Science Foundation through the Cornell Center for Materials Research and by DARPA. Additional support provided by NSF through use of the National Nanofabrication Users Network.

[1] K. Bussman, G. A. Prinz, S. F. Cheng, and D. Wang, Appl. Phys. Lett. **75**, 2476 (1999).
[2] J. A. Katine, F. J. Albert, and R. A. Buhrman, Appl. Phys. Lett. **76**, 354 (2000).
[3] L. Berger, Phys. Rev. B **54**, 9353 (1996).
[4] J. C. Slonczewski, J. Magn. Magn. Mater. **159**, L1 (1996).
[5] Ya. B. Bazaliy, B. A. Jones, and S.-C. Zhang, Phys. Rev. B **57**, R3213 (1998).
[6] X. Weintal, E. B. Myers, Piet W. Brouwer, and D. C. Ralph, cond-mat/0005251 (unpublished).
[7] M. Tsoi, A. G. M. Jansen, J. Bass, W. C. Chiang, M. Seck, V. Tsoi, and P. Wyder, Phys. Rev. Lett. **80**, 4281 (1998); **81**, 493 (1998) (E).
[8] E. B. Myers, D. C. Ralph, J. A. Katine, R. N. Louie, and R. A. Buhrman, Science **285**, 867 (1999).
[9] J. A. Katine, F. J. Albert, R. A. Buhrman, E. B. Myers, and D. C. Ralph, Phys. Rev. Lett. **84**, 3149 (2000).
[10] J. Z. Sun, J. Magn. Magn. Mater. **202**, 157 (1999).
[11] C. R. P. Cowburn, C. K. Koltsov, A. O. Adeyeye, and M. E. Welland, Phys. Rev. Lett. **83**, 1042 (1999).
[12] F. Schreiber, J. Phlaum, Z. Frait, T. Muhge, and J. Pelzl, Solid State Commun. **93**, 965 (1995).
[13] M. R. McCartney, R. E. Dunin-Borkowski, M. R. Scheinfein, D. J. Smith, S. Gider, and S. S. P. Parkin, Science **286**, 1337 (1999).